European Organization for Nuclear Research

CERN

p_{T} spectra and multiplicity vs centrality in Pb-Pb collisions at $\sqrt{s_{NN}} = 5.02$ TeV

Author:
Òscar Lara

Supervisors:
Antonio Ortiz and Guy Paic

Report corresponding to the CERN Summer Program 2021

September 2021

Contents

1 Introduction

The Standard Model (SM) of particle physics is a Quantum Field Theory based on the principles of Lorentz invariance, Gauge invariance and Renormalizability. It describes almost all particle physics phenomena to a never expected precision.

The SM explains three of the four fundamental interactions: electromagnetic, weak and strong, not including gravity yet. We will be focusing on the strong force, described by a theory called Quantum Chromodynamics (QCD).

In this work we will be working with heavy ion collisions, hence a good way to start would be to motivate the need to study ultra-relativistic heavy ion collisions. The key point is that when we have a collision of heavy ions, they recreate the droplets of matter that were present in the universe shortly after the Big Bang happened, when the universe was just a a few microseconds old. At this early stage of the universe, the present matter was at higher temperatures than Λ_{QCD} (see Ref.[1]) what prevented hadrons to have formed meaning that the quarks and gluons present at that time could not be described as a collection of hadrons. However, the quarks and gluons were not independent from each other, they were strongly coupled to each other, a form of matter that has received the name Quark-Gluon Plasma (QGP). At ALICE (A Large Ion Collider Experiment), these conditions are achieved with the use of heavy ion collisions.

These collisions can be studied from different perspectives, however in this report we will be studying transverse momentum (p_T), centrality and event multiplicity, quantities that will be defined later.

The ALICE experiment at the LHC (Large Hadron Collider) reconstructs and identifies particles in proton-proton (pp), proton-lead (p-Pb) and lead-lead (Pb-Pb) collisions[1], for a wide range of p_T. As discussed in Ref.[2] the main central detectors are Inner Tracking System (ITS), Time Projection Chamber (TPC), Transition Radiation Detector (TRD), Time Of Flight (TOF) and ElectroMagnetic CALorimeter (EMCAL), but we will be working with the V0 detector, a forward detector.

To study these heavy ion collisions, it is useful to introduce a quantity called *centrality*, defined as the percentile of the hadronic cross section corresponding to a particle multiplicity, or an energy deposited, measured in ALICE, above a given threshold (N_{ch}^{THR}) (Ref.[3])

$$c = \frac{1}{\sigma_{AA}} \int_{N_{ch}^{THR}}^{\infty} \frac{d\sigma}{dN'_{ch}} dN'_{ch} = \frac{1}{\sigma_{AA}} \int_{0}^{E_{ZDC}^{THR}} \frac{d\sigma}{dE'_{ZDC}} dE'_{ZDC} \tag{1}$$

[1]In this work we will only study Pb-Pb collisions

Originally in our analysis we will be working with 6 centrality classes, $0-5\%, 5-10\%, 10-20\%, 20-40\%, 40-60\%, 60-90\%$, where the $0-5\%$ centrality class corresponds to the most central collisions and the $60-90\%$ centrality class corresponds to the most peripheral collisions.

We we would also like to define the *multiplicity* of a collision as the number of particles that have been produced and the *transverse momentum* p_T as the component of the momentum perpendicular to the beam line.

2 Analysis

We will be using Pb-Pb collisions data collected by ALICE at $\sqrt{s_{NN}} = 5.02$ TeV. The used data corresponds to the period LHC15n pass 4, runs: 244628, 244484, 244377, 244627, 244483, 244364, 244626, 244482, 244359, 244619, 244481, 244355, 244618, 244480, 244351, 244617, 244456, 244343, 244542, 244453, 244340.

We will be using and modifying an analysis code provided by the supervisors at ICN-UNAM, an analysis that we will proceed to explain.

2.1 Program

In this section we will very briefly explain the basics of the code that we will be using to perform our analysis, in order to be able to highlight the changes that have been done to this analysis (Section 2.2) to obtain our results (Section 3).

First we should mention how events are selected at ALICE [4]. First, the minimum-bias trigger requires signals in both the V0A and the V0C detectors, after which an offline event selection is applied to remove beam-induced background and pileup events. Pileup events are removed by comparing multiplicity estimates from the V0 detector to those of tracking detectors at mid-rapidity. Then, centrality is estimated from the energy deposition measured in the V0 detector.

To start our analysis, we iterate over all the events, and for each one of these events we apply 7 conditions, if a certain event does not fulfill a certain condition, we discard it. This process is represented in Fig. 1.

Then, for each one of these events we get its centrality class, the number of tracks produced, and we iterate again over the number of tracks produced at each event. For each one of the tracks, we can get its p_T, a quantity that we store in a histogram

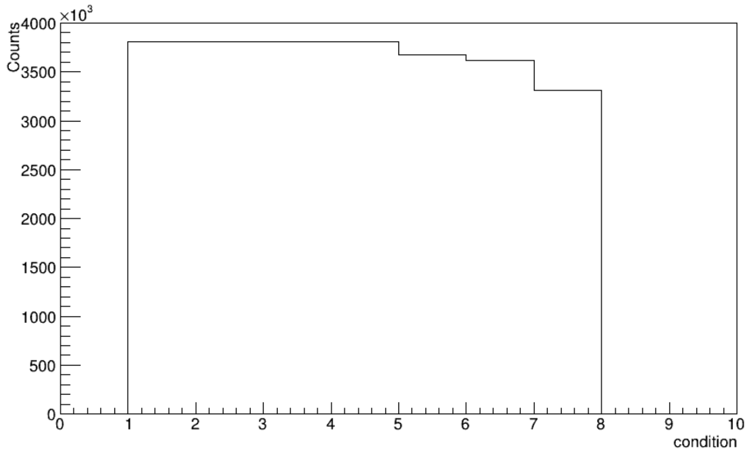

FIGURE 1: Visualizations of the process of imposing conditions on the events

depending on the centrality class that corresponded to that event. To summarize, what we obtain is:

- A multiplicity histogram, that counts the number of times that an event had a particular multiplicity. We have one of this histograms for each centrality class.
- A p_T histogram, that counts the the number of times that a produced track had a certain p_T. We also have one of this histograms for each centrality class.

2.2 Updates

As explained in Section 1, we were provided an analysis with 6 centrality classes, $0-5\%, 5-10\%, 10-20\%, 20-40\%, 40-60\%, 60-90\%$. However, as a first part of this project we implemented thinner centrality classes, and actually increased the number of centrality classes to 90, therefore obtaining the centrality classes $0-1\%, 1-2\%, ..., 89-90\%$. In this report we will be presenting results for both the original centrality classes (6 centrality classes) and for the new centrality classes (90 centrality classes).

Furthermore, the low and high multiplicity parts of each centrality class were separated. The procedure followed for each centrality class was:

- As we already explained, we obtained a multiplicity histogram.
- We obtained the mean μ and the standard deviation σ of the multiplicity histogram.

- We ran the program again, but now separating the low and high multiplicity parts. If we let m be the multiplicity of a certain event, we classify this event as low multiplicity if $m < \mu - \sigma$ and high multiplicity if $m > \mu + \sigma$.

This procedure can be visualized in Fig.2.

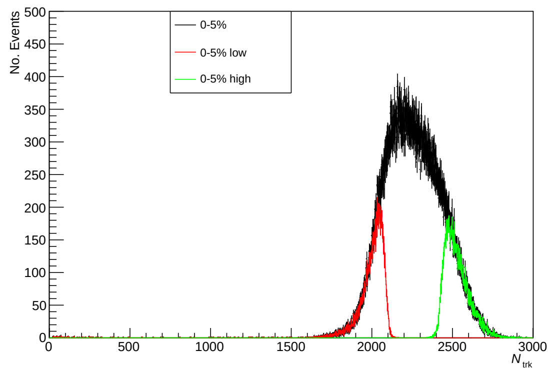

FIGURE 2: Separating low and high multiplicity for the $0 - 5\%$ centrality class. In black we have the whole distribution, in red we have the low multiplicity part of the distribution and in green we have the high multiplicity part.

Moreover, since we could classify events into low and high multiplicity, we also separated the p_T distributions into low and high. If a certain event was classified as low multiplicity, then all the p_T's of the corresponding produced tracks were classified as low, and analogously for high multiplicity.

2.3 Ratios

We would like to study the dependence of the p_T distributions with the centrality class, and for this purpose it will be useful to define some ratios. However, first we need to normalize the obtained p_T distributions, we normalize them by the bin width, by the pseudorapidity η and by the total number of events that contributed to that p_T histogram. We will be studying the quantity:

$$\frac{1}{N_{ev}} \frac{d^2N}{dp_T d\eta} \tag{2}$$

Now we will define several ratios, explaining what they represent. First, let us define a ratio R_{aa}^{ij} as

$$R_{aa}^{ij} = \frac{\left(\frac{1}{N_{ev}} \frac{d^2N}{dp_T d\eta}\right)_i}{\left(\frac{1}{N_{ev}} \frac{d^2N}{dp_T d\eta}\right)_j} \tag{3}$$

where i and j are indices that run over the centrality classes. For example $i = 0 \to 0 - 5\%$, $i = 1 \to 5 - 10\%$... if we have 6 centrality classes or $i = 0 \to 0 - 1\%$, $i = 1 \to 1 - 2\%$ if we have 100 centrality classes. The subindices stand for all/all, meaning that we are not separating low and high here. We will be interested in normalizing with respect to the most central collision, therefore we will be studying the ratios R^{i0}_{aa}.

Let us also define the ratio R_{lh}, defined for each centrality class as

$$R_{lh} = \frac{\left(\frac{1}{N_{ev}}\frac{d^2N}{dp_T d\eta}\right)_{low}}{\left(\frac{1}{N_{ev}}\frac{d^2N}{dp_T d\eta}\right)_{high}} \tag{4}$$

This represents the ratio of the p_T of the low multiplicity part over the high multiplicity part. We have one of this ratios for each centrality class.

We also define the ratio R^{ij}_{hh}, which is similar to R^{ij}_{aa} but we only take into account the high multiplicity part

$$R^{ij}_{hh} = \frac{\left(\frac{1}{N_{ev}}\frac{d^2N}{dp_T d\eta}\right)_{i,high}}{\left(\frac{1}{N_{ev}}\frac{d^2N}{dp_T d\eta}\right)_{j,high}} \tag{5}$$

and the same quantity for low/low.

Finally, we will also be interested in the quantity R^{i0}_{hh}, putting the most central distribution in the denominator. Finally, we will be studying the overlap region between two different centrality classes. By that we mean the region in which two different centrality classes have similar multiplicities, as it can be visualized in Fig.3, where the overlap region is formed by the pink and red distributions. The corresponding ratio is defined as

$$R_{overlap} = \frac{\left(\frac{1}{N_{ev}}\frac{d^2N}{dp_T d\eta}\right)_{red}}{\left(\frac{1}{N_{ev}}\frac{d^2N}{dp_T d\eta}\right)_{pink}} \tag{6}$$

3 Results

3.1 Multiplicity

We are now ready to look at the results of our analysis, starting first for the multiplicity histograms, that can be seen in Fig.4. The first remark that we want to make is that for the thinner centrality classes we get less events than for the original centrality classes. This is logical since the centrality classes $0 - 1\%, 1 - 2\%, 2 - 3\%, 3 - 4\%$ and $4 - 5\%$ are

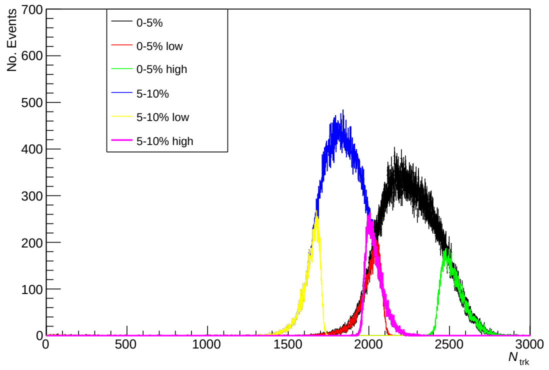

FIGURE 3: Definition of the overlap region between the $0-5\%$ and $5-10\%$ centrality classes. For this discussion we have only considered the red and magenta distributions.

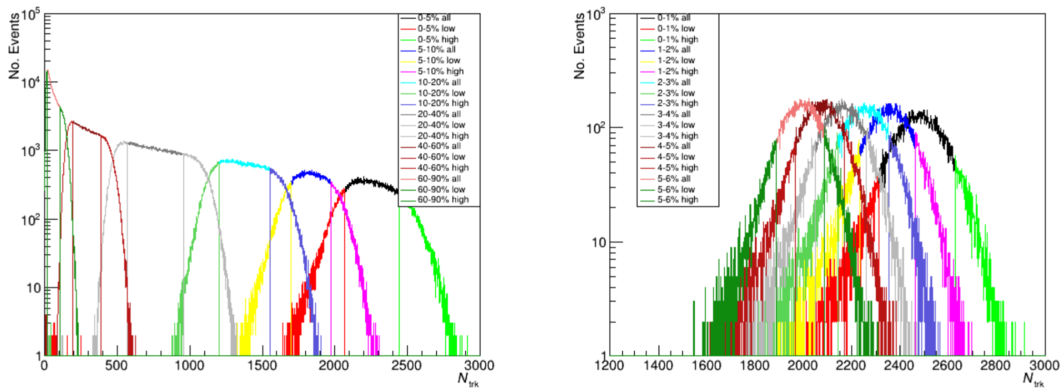

(A) Original centrality classes.

(B) Thinner centrality classes.

FIGURE 4: Multiplicity histograms for different centrality classes.

inside the centrality class $0-5\%$. The centrality class $0-5\%$ has $N_{trk} \in (1650, 2800)$, that agrees with the lowest multiplicity of the centrality class $4-5\%$ being around[2] 1700 tracks and the highest multiplicity of the centrality class $0-1\%$ being around 2850 tracks.

In Fig.4a we also observe that the number of events increases as we go to more peripheral collisions.

We can go further and plot the multiplicity results for even thinner centrality classes: $0.0-0.1\%, 0.1-0.2\%, ..., 0.4-0.5\%$, as seen in Fig.5. We observe that for this case we have really low statistics. Furthermore, the conclusion that we can get from all the multiplicity results is that the spread in multiplicity of $0-5\%$ is not very different from

[2]Notice that the distributions for thinner centrality classes are less clear since we have less data.

the $0-1\%$ and $0.0-0.1\%$ spreads, a result that needs to be further studied but we believe that it is caused by the partons that irradiate other partons when produced.

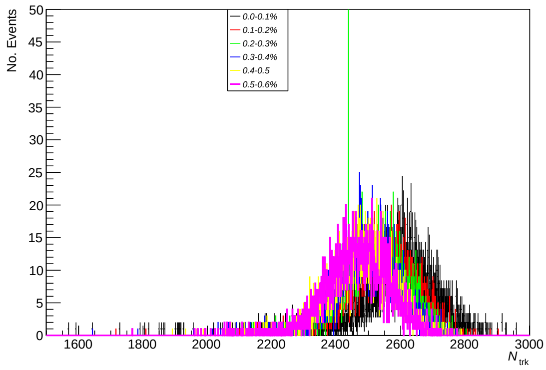

FIGURE 5: Multiplicity distributions for $0.0-0.1\%, ..., 0.5-0.6\%$ centrality classes.

3.2 Ratios

We can now discuss the obtained results for the different ratios introduced in Section 2.3. We will first discuss the original centrality classes $0-5\%, 5-10\%, 10-20\%, 20-40\%, 40-60\%, 60-90\%$ and then the thinner centrality classes $0-1\%, 1-2\%, ..., 89-90\%$.

3.2.1 Original centrality classes

First, we can look at Fig.6, where we observe the results for R_{aa}^{i0}, defined in Eq.(3). The first thing to note is that for the most central centrality class we obtain R_{aa}^{00} as it should be since we put the same quantity in the numerator and in the denominator. Moreover, we observe a suppression of high p_T particles for the most central collision with respect to the less central, since at around $p_T = 5$ GeV/c the ratios increase.

Let us now look at the results for R_{lh}, defined in Eq.(4), which can be seen in Fig.7. We observe an approximately constant trend, a constant that depends on the difference in multiplicities for the low and high distributions. Something remarkable is that for high p_T we observe a slight suppression of low multiplicity events, since we observe a decrease in the ratio. A remarkable feature of Fig.7 is that we observe a maximum at around $p_T = 2$ GeV/c for the semicentral centrality classes ($20-40\%$ and $40-60\%$), what reminds us of the shape of the RAA nuclear modification factor, see for example Ref.[4] for more details. For this reason in Fig.8 we have plotted the inverse of Fig.7, to actually observe the shape observed at Ref.[4]. This needs to be studied further.

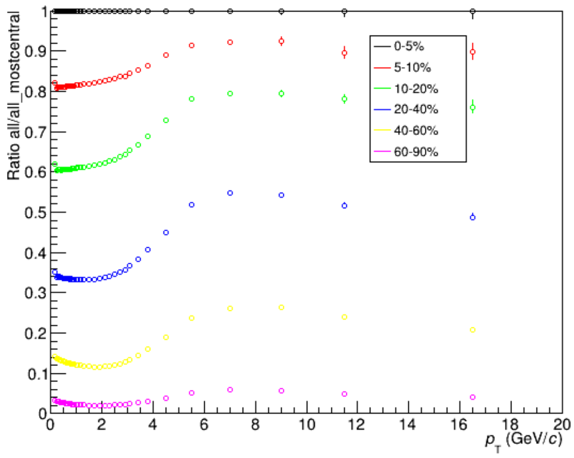

FIGURE 6: R_{aa}^{i0}, defined in Eq.(3). This represents the ratio of the different p_T distributions normalized to the distribution of the most central centrality class.

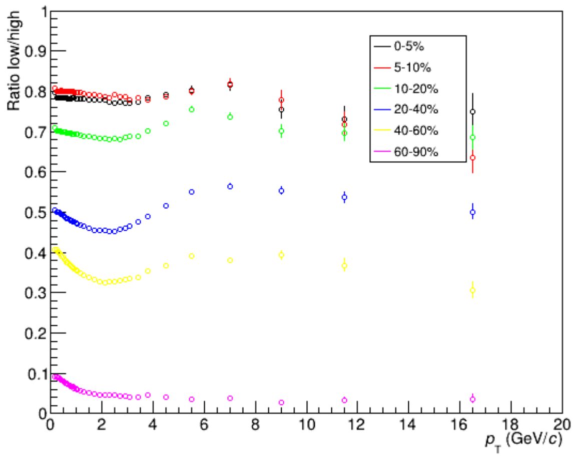

FIGURE 7: R_{lh}, defined in Eq.(4). This represents the ratio of the p_T distributions of the low and high part of the same centrality class.

In Figures 9 and 10 we have plotted R_{hh}^{ij} and R_{ll}^{ij}, as defined in Eq.(5). The main feature of these ratios is that their shapes are actually really similar to the one we observe in Fig.6. However, for peripheral centrality classes we observe that the ratio low/low is smaller than the ratio high/high.

Finally we can discuss the results for $R_{overlap}$, that can be seen in Fig.11. We have already seen, for example in Fig.3 that the p_T distributions depend on the centrality class, which depends on the multiplicity. However, is it possible that the p_T distributions depend only the multiplicity and not on the centrality class? This is why we study $R_{overlap}$, to study different centrality classes that have the same multiplicity. If we measured $R_{overlap} = 1$ it would mean that the p_T distributions depend only on the multiplicity

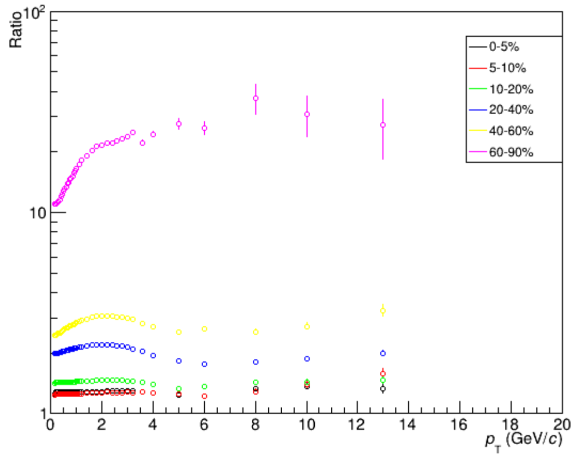

FIGURE 8: Inverse of Fig.7, R_{hl}, to observe a similar effect as in R_{AA}.

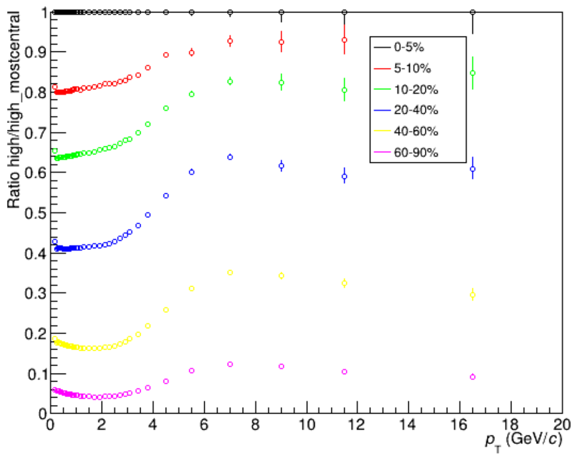

FIGURE 9: R^{ij}_{hh}, defined in Eq.(5). This represents the ratios of the p_T distributions of the high multiplicity part, normalized with the one from the most central centrality class.

(and the dependence on the centrality class would be fictitious, since different centrality classes have different multiplicities). Nevertheless, this is not what we observe in Fig.11, we observe that we are getting $R_{overlap} \neq 1$.

3.2.2 Thinner centrality classes

Now we would like to focus our attention to the thinner centrality classes: $0-1\%, 1-2\%, ..., 89-90\%$. We will study exactly the same quantities and in the same order as we did for the original centrality classes.

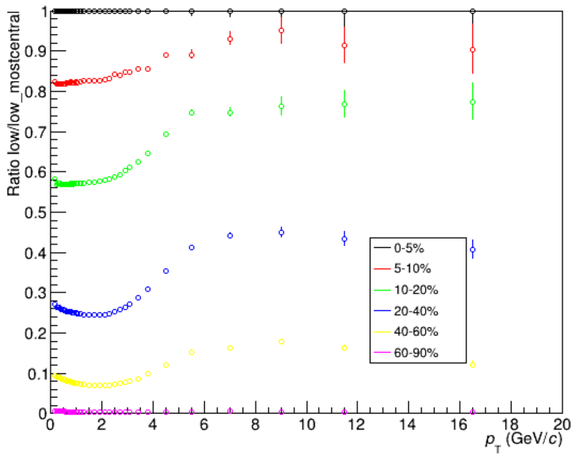

FIGURE 10: R^{ij}_{ll}, defined in Eq.(5). This represents the ratios of the p_T distributions of the low multiplicity part, normalized with the one from the most central centrality class.

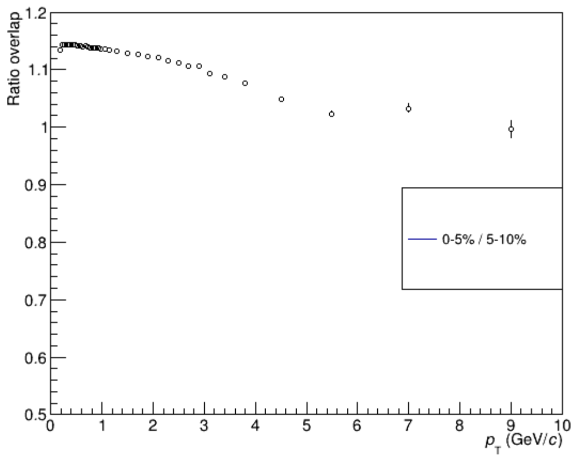

FIGURE 11: $R_{overlap}$, defined in Eq.(6). This represents the ratio of two distributions that have approximately de same multiplicity but different centrality.

First let us look at the ratios all/all plotted in Figure 12 for central centrality classes and for semi-central centrality classes. We can appreciate a similar pattern to the one we observed in Fig.6, an increase in the ratio at around 2 GeV/c and then the ratio is stable to a constant. We would also like to mention that for high p_T the uncertainties on the thinner centrality classes get bigger, since for the thinner centrality classes we have less statistics. We alos want to mention that we have always normalized to the centrality class $0 - 1\%$, this is the reason why the ratio is not 1 for the centrality class $20 - 21\%$, in Fig.12b.

In Fig.13 we can observe the low/high ratios for the thinner centrality classes, plots

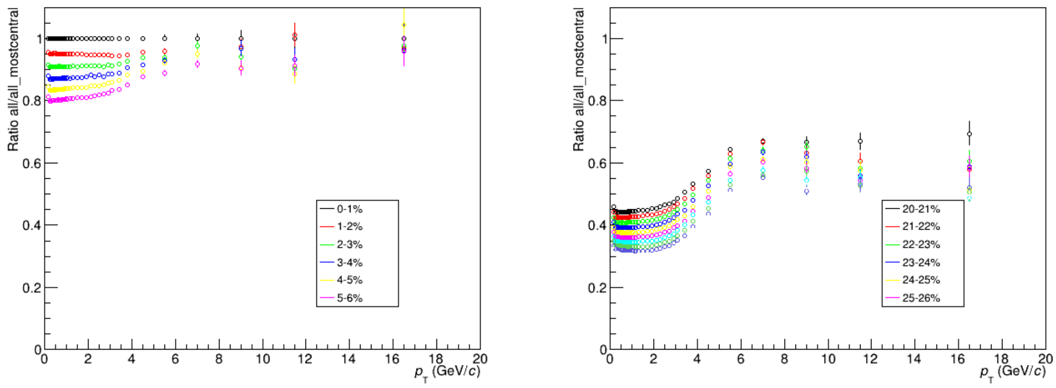

(A) Original centrality classes.

(B) Thinner centrality classes.

FIGURE 12: R_{aa}^{i0}, defined in Eq.(3). This represents the ratio of the different p_T distributions normalized to the distribution of the most central centrality class.

that are analogous to Fig.7. We observe some differences, first of all we would like to mention that the most central collision does not have the biggest ratio in this case, as it happened in the original centrality classes. Also, we want to mention that it is really difficult to disentangle the different centrality classes since they are really similar, specially at high p_T where we have bigger errorbars.

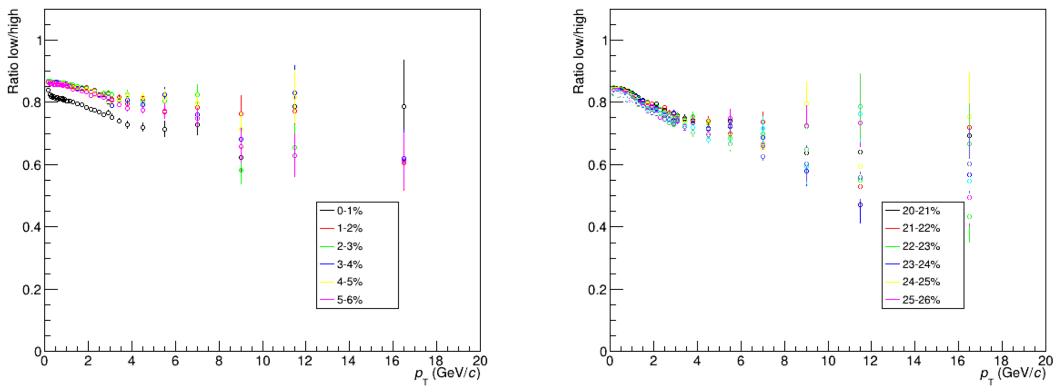

(A) Central sector of the thinner centrality classes

(B) Peripheral sector of the thinner centrality classes

FIGURE 13: R_{lh}, defined in Eq.(4). This represents the ratio of the p_T distributions of the low and high part of the same centrality class.

Finally, in Figures 14 and 15 we have the high/high and low/low plots, analogously to Figures 9 and 10. We observe that the shapes of the plots are similar to the ones we observed for the original centrality classes. However, the numerical values are different, as our intuition expects.

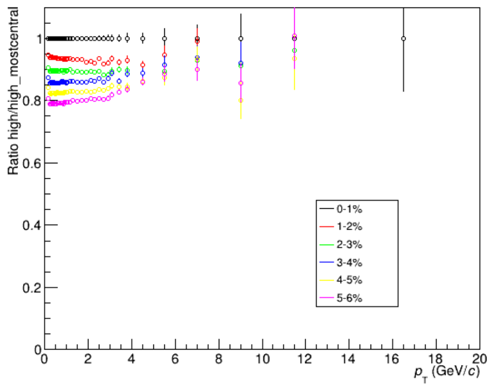

(A) Central sector of the thinner centrality classes

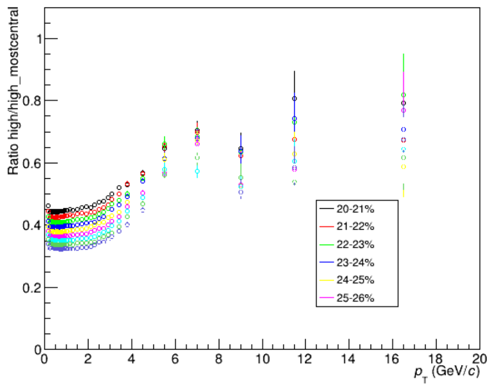

(B) Peripheral sector of the thinner centrality classes

FIGURE 14: R^{ij}_{hh}, defined in Eq.(5). This represents the ratios of the p_T distributions of the high multiplicity part, normalized with the one from the most central centrality class.

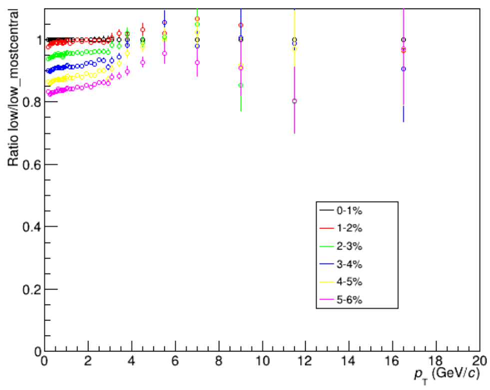

(A) Central sector of the thinner centrality classes

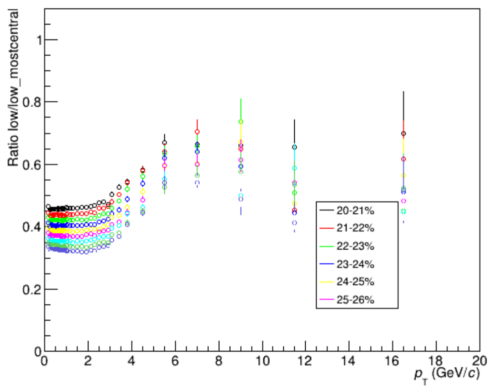

(B) Peripheral sector of the thinner centrality classes

FIGURE 15: R^{ij}_{ll}, defined in Eq.(5). This represents the ratios of the p_T distributions of the low multiplicity part, normalized with the one from the most central centrality class.

4 Conclusions

Studying heavy ion collisions at the LHC is extremely important to understand Quark-Gluon Plasma, a form of matter present in the early universe, and it can help us achieve a better understanding of nature.

In this project we have focused on the multiplicity and p_T distributions for Pb-Pb collisions at ALICE, trying to study how this quantities depend on the considered centrality class.

First, we have implemented thinner centrality classes ($0-1\%, ..., 89-90\%$), and we have studied the multiplicity distributions of these centrality classes, observing that we get more events for the peripheral collisions, but the main conclusion that we want to mention is that the spreads in multiplicity are really similar for the original and thinner centrality classes, something that had not been studied before.

Then, we have defined and studied several ratios of the p_T distributions, highlighting its interesting features. Two important conclusions that we would like to remark is that we observed a suppression of low multiplicity events for high p_T in the ratios all/all, and that in the ratios low/high we observed a behaviour really similar to that of the R_{AA}. However, this should be further studied. We would also like to mention that we have observed a difference between the low/low and high/high ratios with respect to the low/high ratios, a remarkable finding that could be explored more.

We have also tested that the dependence of the p_T distributions is on the centrality class and not on the multiplicity, since we studied two different centrality classes that have the same multiplicity, but we got different results.

5 Acknowledgements

I would like to thank my supervisors Guy Paic and Antonio Ortiz. Working under your supervision has been a really enriching experience, and I have definitely learned a lot from you.

I would also like to thank CERN and the CERN Summer Program Team for organizing the Summer Program, it is an amazing experience for students to be able to participate in a project and to attend all the events that you have prepared for us.

Bibliography

[1] W. Busza, K. Rajagopal, and W. Van Der Schee, "Heavy ion collisions: the big picture and the big questions," *Annual Review of Nuclear and Particle Science*, vol. 68, pp. 339–376, 2018.

[2] K. Aamodt, A. A. Quintana, R. Achenbach, S. Acounis, D. Adamová, C. Adler, M. Aggarwal, F. Agnese, G. A. Rinella, Z. Ahammed, *et al.*, "The ALICE experiment at the CERN LHC," *Journal of Instrumentation*, vol. 3, no. 08, p. S08002, 2008.

[3] ALICE Collaboration, "Centrality determination in heavy ion collisions," tech. rep., ALICE-PUBLIC-2018-011, 2018.

[4] S. Acharya, D. Adamová, J. Adolfsson, M. Aggarwal, G. A. Rinella, M. Agnello, N. Agrawal, Z. Ahammed, S. Ahn, S. Aiola, *et al.*, "Anisotropic flow of identified particles in pb-pb collisions at $\sqrt{s_{\mathrm{NN}}} = 5.02$ TeV.," *Journal of High Energy Physics*, vol. 2018, no. 9, pp. 1–46, 2018.